One-Step Detection of Pathogens and Viruses: Combining Magnetic Relaxation Switching and Magnetic Separation

Yiping Chen,[†,‡] Yunlei Xianyu,[†,‡] Yu Wang,[§] Xiaoqing Zhang,[†] Ruitao Cha,[†] Jiashu Sun,[*,†] and Xingyu Jiang[*,†]

[†]Beijing Engineering Research Center for BioNanotechnology and CAS Key Laboratory for Biological Effects of Nanomaterials and Nanosafety, National Center for NanoScience and Technology, Beijing, 100190, China and [§]Beijing Institute for Tropical Medicine, Beijing Friendship Hospital, Capital Medical University, 95 Yongan Road, Xicheng District, Beijing, 100050, China. [‡]Y. Chen and Y. Xianyu contributed equally.

ABSTRACT We report a sensing methodology that combines magnetic separation (MS) and magnetic relaxation switching (MS-MRS) for one-step detection of bacteria and viruses with high sensitivity and reproducibility. We first employ a magnetic field of 0.01 T to separate the magnetic beads of large size (250 nm in diameter) from those of small size (30 nm in diameter) and use the transverse relaxation time (T_2) of the water molecules around the 30 nm magnetic beads (MB_{30}) as the signal readout of the immunoassay. An MS-MRS sensor integrates target enrichment, extraction, and detection into one step, and the entire immunoassay can be completed within 30 min. Compared with a traditional MRS sensor, an MS-MRS sensor shows enhanced sensitivity, better reproducibility, and convenient operation, thus providing a promising platform for point-of-care testing.

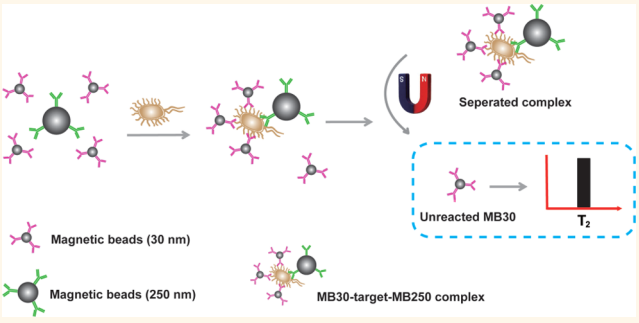

KEYWORDS: magnetic relaxation switch · magnetic separation · magnetic bead · one-step detection · homogeneous immunosensor

Rapid detection of pathogens and viruses with high sensitivity is essential for timely clinical decision-making and management of epidemics of infectious diseases.[1−5] Many approaches have been developed for pathogen detection, including the enzyme-linked immunosorbent assay (ELISA),[6,7] the gold lateral flow strip (GLFS),[8] polymerase chain reaction (PCR),[9,10] and so forth. ELISA and GLFS are widely used methods for pathogen detection due to their good specificity, low cost, and straightforward readout. However, the sensitivity still remains a great challenge when it comes to early diagnosis of pathogen infection. In addition, ELISA is often time-consuming and labor-intensive, which limits its application in point-of-care testing (POCT). For pathogen identification at the molecular level, PCR is adopted as the gold standard. Although PCR enables pathogen detection with high sensitivity, it requires expensive instrumentation and skilled technicians, which limit its applications in resource-poor settings, where acute infections often take place. Therefore, it is urgent to develop a rapid, highly sensitive, and low-cost approach that allows point-of-care detection of pathogens and viruses.

Recently, magnetic relaxation switching (MRS) assays that employ target-induced aggregation (or disaggregation) of magnetic beads (MBs) are used to detect a wide range of biomolecules.[11−14] In an external uniform magnetic field, the existence of the target in the sample will result in the state change of antibody-conjugated MBs (from a dispersed state to an aggregated state), thus leading to a local heterogeneous magnetic field. The local magnetic field alters the transverse relaxation time (T_2) of the surrounding water molecules, and the change of the ΔT_2 value (the change of T_2) is related to the degree of aggregation of the MBs, which is dependent on the amount of target in the sample. The ΔT_2 value can

* Address correspondence to xingyujiang@nanoctr.cn, sunjs@nanoctr.cn.

Received for review January 12, 2015 and accepted March 5, 2015.

Published online March 06, 2015
10.1021/acsnano.5b00240

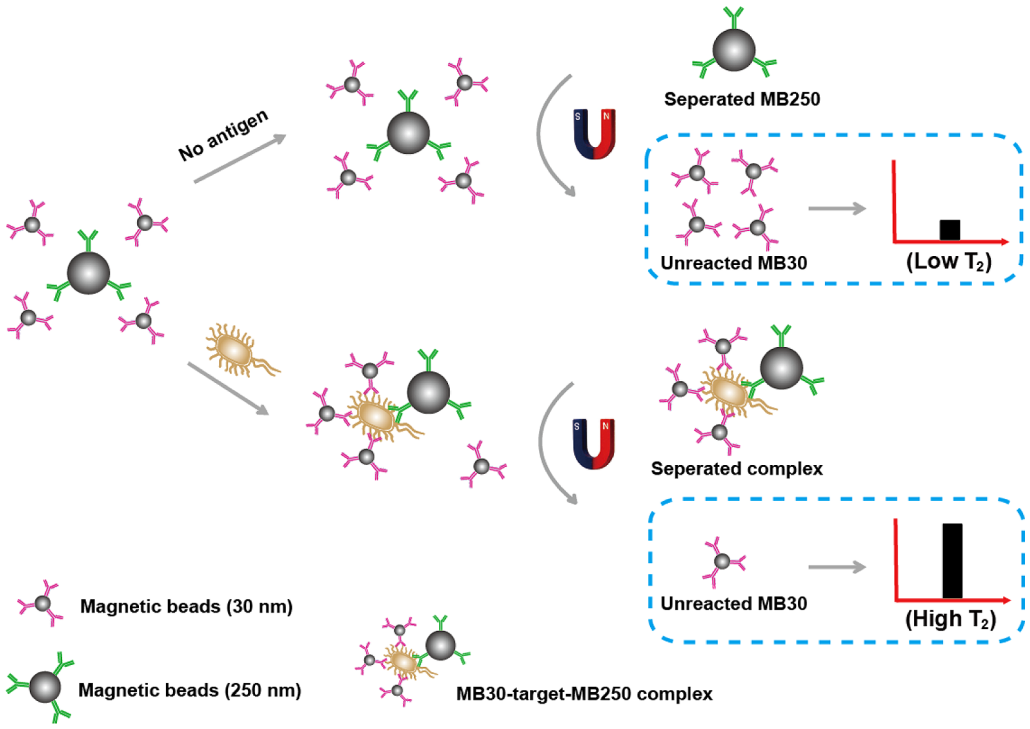

Scheme 1. Schematic illustration of the MS-MRS sensor. MB_{250} and MB_{30} can selectively capture and enrich the target to form the sandwich "MB_{250}-target- MB_{30}" conjugate. After the magnetic separation, the T_2 signal of water molecules around the unreacted MB_{30} can be employed as the readout.

thus be used as magnetic signal readout in the MRS assay. Compared to colorimetric and fluorescent assays, the MRS-based assay is homogeneous, light-independent,[15−17] and easy to operate without laborious pretreatment and purification. Because most biological and environmental samples intrinsically have a low magnetic background,[18] the MRS-based approach requires only simple or even no pretreatment of samples without compromising the sensitivity.[19,20] In the past three years, the working mechanism of an MRS sensor has been systematically investigated,[21] which is helpful to explore this sensor in the field of biochemical analysis. Meanwhile, the combination of an MRS sensor with microfluidics[22,23] or a "click chemistry" signal amplification system[24−26] has significantly improved the sensitivity and portability of the assay. Nevertheless, conventional MRS assays based on target-induced aggregation (or disaggregation) of MBs still suffer from the following limitations: (1) The conventional MRS sensor has two analytical modes, and it is not easy to choose the suitable mode, which correlates with many factors, such as the type of targets[27] and the core size of the MBs.[21] (2) The magnetic signal of a conventional MRS sensor depends on the state change of MBs (from a dispersed state to an aggregated state) through antibody−antigen recognition, but the state of the MBs does not change in some cases, resulting in a reduced signal-to-noise ratio and the loss of sensitivity.[21,28] (3) The concentration ratio between the target and the MBs also affects the stability and the linear range of the detection (this ratio often has to fall within a certain range for an effective analysis); sometimes this ratio is not suitable and sacrifices sensitivity and accuracy. This problem is called the "prozone effect" in a conventional MRS-based assay.[17] Therefore, it is necessary and of great value to develop a sensing methodology that can circumvent the above-mentioned limitations of a conventional MRS sensor.

In this study, we present a sensitive, rapid, and robust MRS-based sensing approach based on magnetic separation (MS) for bacteria and viruses detection with a straightforward operation. The approach exploits the phenomenon that a small magnetic field (0.01 T) can separate MBs of large size (250 nm, abbreviated as MB_{250}) from those of small size (30 nm, abbreviated as MB_{30}). MB_{250} can be rapidly separated by this small magnetic field (0.01 T) in 1 min due to its high saturation magnetization. In comparison, MB_{30}, which is used as the magnetic probe of MRS in this study, cannot be separated by the same magnetic field even after 60 min because of its low saturation magnetization. Based on the great difference in the separation speed of MB_{30} and MB_{250}, we propose a novel strategy for MRS sensing by using the transverse relaxation time (T_2) of MB_{30} as the readout (Scheme 1). In this strategy, both MB_{30} and MB_{250} are conjugated with antibodies that can specifically recognize the different epitopes of the target. The MB_{250} can capture and enrich the target (bacteria or virus) from complicated samples, followed by the binding of MB_{30}

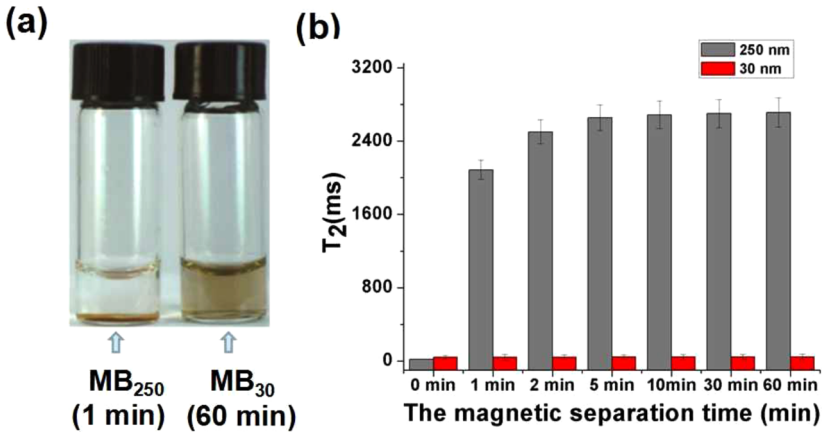

Figure 1. (a) Different magnetic separation speeds between MB_{250} and MB_{30} under the same magnetic field (0.01 T). The MB_{30} is well dispersed in the magnetic field (after 60 min), and the MB_{250} is precipitated to the bottom of the vial (after 1 min) in the same magnetic field. The concentrations of MB_{250} and MB_{30} are both 500 μg/mL. (b) Relationship between the T_2 values of MB_{250} and MB_{30} and magnetic separation time. The magnetic separation time is from 0 to 60 min.

through antibody−antigen recognition, resulting in a "sandwich" immunocomplex (MB_{250}-target-MB_{30}). We use a constant, excess amount of MB_{30} and employ the unreacted MB_{30} as the magnetic signal probe for readout, provided that the MB_{250}-target-MB_{30} can be rapidly removed by the magnetic separation (0.01 T). The T_2 value depends on the amount of the unreacted MB_{30}, and the amount of target inversely correlates with the amount of the unreacted MB_{30}, which in turn results in a different T_2 for the target detection. When no target exists, due to the lack of immunoreaction, the excess amount of unreacted MB_{30} leads to a low T_2 value. On the other hand, the introduction of a target triggers the immunoreaction, resulting in a reduced amount of unreacted MB_{30} and a high T_2.

RESULTS AND DISCUSSION

Mechanism of the MS-MRS Sensor. In our experiment, we exploit the difference of separation speed between MB_{250} and MB_{30} in the same magnetic field (Figure 1a). MB_{30} is well dispersed in the magnetic field (after 60 min) due to its low saturation magnetization, whereas MB_{250} of high saturation magnetization is rapidly precipitated to the bottom of the vial under the same magnetic field (0.01 T, after 1 min). The time course measurement of the T_2 value of the water molecules in the presence of MB_{250} and MB_{30} also proves the different magnetic separation speeds between the MB_{250} and MB_{30} under the same magnetic field (Figure 1b). The T_2 values from the MB_{30} solution at different magnetic separation time points (from 1 to 60 min) do not differ significantly. In contrast, the T_2 value of the MB_{250} solution at the 0 min point is much smaller than that of other time points (from 1 to 60 min), which indicates that the MB_{250} solution can be rapidly aggregated to the bottom (within 2 min). Antibody-conjugated MB_{250} and MB_{30} can selectively capture and enrich the target to form MB_{250}-target-MB_{30} *via* antibody−antigen reaction. MB_{250}-target-MB_{30} can be removed by means of magnetic separation. We set the total amount of MB_{30} constant, so that the unreacted MB_{30} reflects the target concentration. The amount of unreacted MB_{30} determines the T_2 value of the surrounding water molecules. T_2 increases when the concentration of the MB_{30} decreases. Because the concentration of unreacted MB_{30} is inversely correlated to the target concentration, the T_2 value can be employed for the quantification of the target (Figure 2b). Since the T_2 value is very sensitive to the concentration of MB_{30}, this MS-MRS is expected to have a high sensitivity. We also use magnetic resonance imaging (MRI) to characterize the performance of MS-MRS. The brightness of the T_2 images gradually decreases when the concentration of *S. enterica* decreases from 10^7 cfu/mL to 0 cfu/mL, because the T_2 value decreases with decreasing concentration of *S. enterica* (Figure S1). The negative sample without *S. enterica* shows the lowest level of brightness (Figure S1). This result further proves the formation of the "MB_{250}-target- MB_{30}" conjugate as a result of the immunoreaction between antibody-conjugated MB and *S. enterica*.

Optimization of the MS-MRS Sensor. We optimized two factors to improve the analytical performances of the MS-MRS sensor, including (1) the size of the MB, which influences the sensitivity and stability, and (2) the concentration of the MBs, which affects the magnetic signal intensity and the linear range.

We optimized the sizes of the MB by testing MB_{20}, MB_{30}, and MB_{50} to reach the optimal sensitivity and stability, as previous work has reported.[21] Among three kinds of MBs of different sizes, we chose MB_{30} to balance the sensitivity and stability. Although the saturation magnetization of MB_{50} is large, which gives rise to the highest ΔT_2 due to its strong ability to affect the T_2 of the surrounding water, the T_2 value of MB_{50} at 5 min is smaller than the T_2 value at 60 min, suggesting

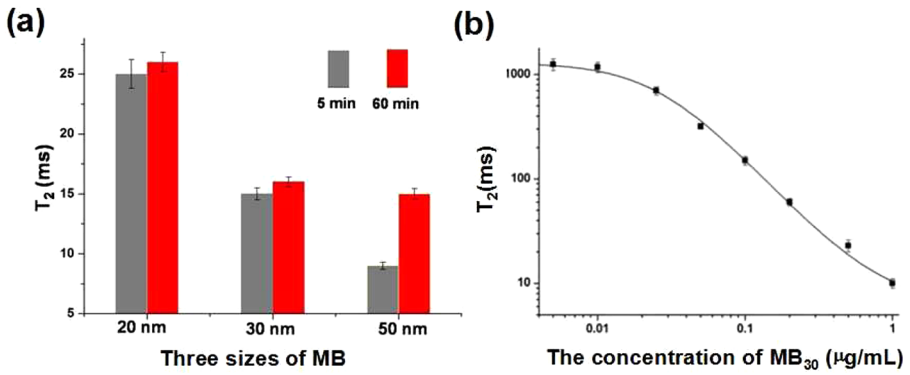

Figure 2. (a) Relationship between the T_2 value and three sizes of MBs (20, 30, and 50 nm) in a magnetic field of 0.01 T. Each 1.5 mL tube has 1 mL of MB (100 μg/mL), which is placed on the magnetic separation rack for 5 and 60 min. At the 5 min point, we collected the supernatant and diluted it by 100-fold by PBS solution for the T_2 measurement. (b) Relationship between the T_2 value and the concentration of MB_{30}. The concentration of MB_{30} is 1, 0.5, 0.2, 0.1, 0.05, 0.025, 0.01, and 0.005 μg/mL.

a weak stability of MB_{50}. By contrast, the T_2 value of MB_{20} becomes similar to that of MB_{30} after 60 min. The reason is that part of the MB_{50} has been separated in the magnetic field, and the concentration of MB_{50} in the supernatant decreases, which will affect the accuracy of the MS-MRS sensor. The sensitivity of the MS-MRS sensor is better using MB_{30} than that with MB_{20}, and the stability of MB_{30} in the magnetic field is as good as that of MB_{20} (Figure 2a). On the basis of the above results, 30 nm MB is the most suitable for construction of the MS-MRS sensor, and we chose MB_{30} for the following experiment.

We optimized the concentration of MB_{30} that would affect the intensity of the magnetic signal and the sensitivity of the assay (Figure S2). According to the sensing mechanism, the unreacted MB_{30} (or the ratio of unreacted MB_{30} to total MB_{30}) partially determines the sensitivity of the MS-MRS sensor. We chose *Salmonella enterica* (*S. enterica*) as the analytical mode in this assay. *S. enterica* is a Gram-negative food pathogen that affects the gastroinstinal tract of exposed individuals and leads to infection, diarrhea, and pain.[29,30] Infection with *S. enterica* causes serious foodborne health problems worldwide, especially in developing countries. When the concentration of MB_{30} is high (10 μg/mL), the MB_{30} captured by the MB_{250}-target is much less than the unreacted MB_{30}, resulting in a negligible ΔT_2 value. On the contrary, when the concentration of MB_{30} is low (0.1 and 0.5 μg/mL), there is not sufficient MB_{30} for target capture, and the ΔT_2 value is not apparent when the concentration of *S. enterica* is 10^6 to 10^7 cfu/mL. On the basis of these results, 1 μg/mL was selected for the subsequent experiments.

Sensitivity and Selectivity of the MS-MRS Sensor. Under the optimized conditions, we evaluated the sensitivity and selectivity of the assay by detecting *S. enterica*. The results show that the ΔT_2 value continuously increases when the concentration of *S. enterica* increases between 10^2 and 10^8 cfu/mL, and the limit of detection (LOD) is 10^2 cfu/mL (Figure 3a). A linear relationship between ΔT_2 and the concentration of *S. enterica* was observed in the range between 10^4 and 10^8 cfu/mL, and the linear equation was $Y = 102.5X - 370$ ($X = \log[C_{S.enterica\ \ concentration}]$, $R^2 = 0.978$) (Figure 3c). We also compared the MS-MRS assay with a conventional MRS assay. For the conventional MRS sensor, the ΔT_2 value increases when the concentration of *S. enterica* is 10^4 to 10^7 cfu/mL (Figure 3b). The LOD of the conventional MRS assay is 10^4 cfu/mL, and the linear detection range is 10^5 to 10^7 cfu/mL. The LOD of the MS-MRS assay decreases by 2 orders of magnitude compared with that of a conventional MRS assay, while the linear detection range increases by 1 order of magnitude.

We explain the better performances of the MS-MRS sensor over the conventional MRS sensor as follows. In this MS-MRS sensor, the concentration of unreacted MB_{30} is related only to the amount of target in the sample, and the ΔT_2 value is very sensitive to the concentration of unreacted MB_{30}, resulting in the good sensitivity and linear detection range. However, in the conventional MRS sensor, the ΔT_2 value depends on the state change of reacted MB_{30} (from dispersed MB_{30} to aggregated MB_{30}-target-MB_{30}). The state of MB_{30} may not change in some cases, which would decrease the signal-to-noise ratio and the sensitivity. In addition, the ΔT_2 value is affected by not only the concentration of *S. enterica* but also other factors such as the type of targets and the size of the MB, leading to the low performance.[27,28]

We also compared our methods with ELISA for the detection of *S. enterica*, because ELISA is a widely used method for pathogen detection due to its high sensitivity and low cost. In this study, we also employ ELISA for the detection of *S. enterica* (Figure S3). The LOD of ELISA for detection of *S. enterica* is 10^3 cfu/mL, and the linear detection range is 5×10^3 to 10^7 cfu/mL. The result shows that the sensitivity of the MS-MRS sensor is better than that of ELISA, and thus it can be used as an ultrasensitive platform for pathogen detection.

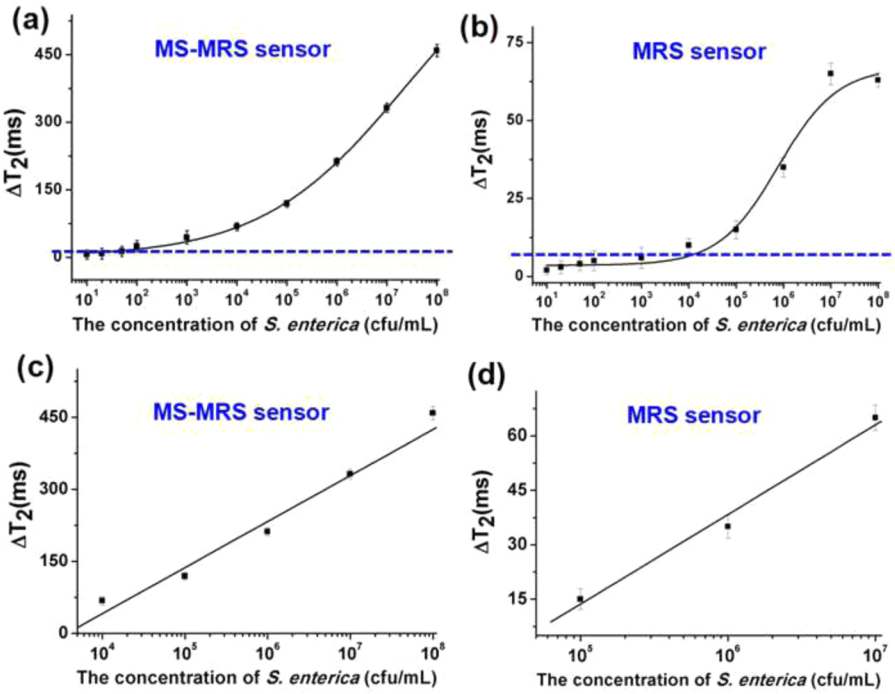

Figure 3. (a and c) Sensitivity and dynamic ranges of an MS-MRS sensor for detection of *S. enterica* in PBS solution. (b and d) Sensitivity and dynamic ranges of a conventional MRS sensor for detection of *S. enterica* in PBS solution. The dashed lines in (a) and (b) show the cutoff values of the MS-MRS sensor and the MRS sensor.

We also investigated the selectivity of the MS-MRS sensor. During the analysis of *S. enterica*, four other bacteria, *E. coli*, *Shigella* spp. (*S.* spp.), *Staphylococcus aureus* (*S. aureus*), and *spirillumcholera* (*S. cholera*), are used to evaluate the selectivity of this sensor (Figure 4). The results show that the ΔT_2 value is remarkably greater in *S. enterica* than other bacteria, suggesting that the sensor has good specificity for *S. enterica* detection. This high selectivity totally depends on the conjugated antibody applied to the MS-MRS assay. If the target is shifted from *S. enterica* to *E. coil*, we may still achieve the high selectivity by adopting the conjugated antibody targeted to *E. coli*. As to the detection range for different targets, the affinity between antibody and antigen may result in the different excessive amounts of unreacted MB30, thus leading to a different detection range.

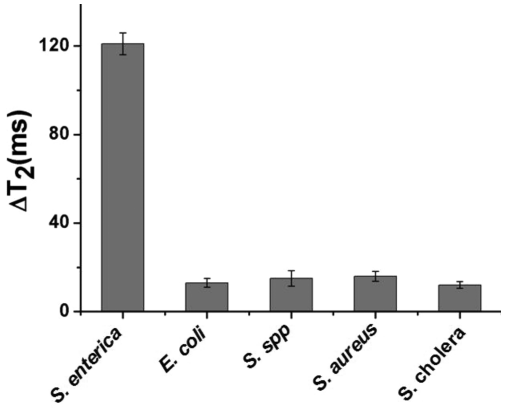

Figure 4. Selectivity of the MS-MRS sensor for detection of *S. enterica*. The concentration of all bacteria is 10^5 cfu/mL.

Repeatability and Operability of the MS-MRS Sensor. Besides the sensitivity and selectivity, operability and repeatability are also two key factors to evaluate a sensor, which largely determine its practical applications. The previous report[21] has indicated that the conventional MRS sensor has two transverse relaxation modes: motional averaging (when the core size of Fe_2O_3/Fe_3O_4 is 8 nm) and static dephasing (when the core size of Fe_3O_4 and $MnFe_2O_4$ is 16 nm, or the core size of Fe_3O_4 is 22 nm), which result in two analysis modes. Moreover, motional averaging can transfer into static dephasing in the MRS sensor. In a typical analysis, it is difficult to know, *a priori*, which mode to use. The analysis modes of a conventional MRS sensor are affected by many factors, such as the stoichiometric ratio between MB and molecular targets, the type of targets, the immunoreaction time, and so forth. Therefore, the choice of suitable analysis mode in conventional MRS is very important, and many experimental conditions should be explored to obtain the optimized results, which greatly affect the accuracy and the operability of conventional MRS. In comparison, there is only one analysis mode in the MS-MRS sensor for detection of biomacromolecules (protein, virus, or pathogen), so that the whole analysis in the MS-MRS sensor is straightforward.

There are mainly two parameters influencing the stability of MBs. One is the size of the MB, and the other is the surface property/chemistry of the MB. Among three kinds of MBs of different sizes ranging

from 20 to 50 nm, we chose an optimal size of 30 nm to balance the sensitivity and stability. As to surface chemistry, the amount of EDC (used in the bioconjugation process) and the conjugated antibody on the surface of the MB can influence the stability of MB_{30}. In our experiment, the MB_{30}-antibody conjugate stored at 4 °C is stable for over six months.

In this MS-MRS sensor, the T_2 value of water molecules around MB_{30} is very stable, which can guarantee the repeatability of the MS-MRS sensor. However, in a conventional MRS sensor, the aggregated MB_{30}-target-MB_{30} conjugate in immunoreactions may become dispersed MB_{30} when the concentration of *S. enterica* reaches a certain point, which results in a change of T_2 value. This may be because the immunoreaction is a dynamic equilibrium reaction,[17] which reduces the accuracy of the MRS sensor. The ΔT_2 value decreases when the concentration of *S. enterica* is 10^7 to 10^8 cfu/mL; the reason may be that the MB_{30}-target-MB_{30} conjugate transfers to the dispersed MB_{30} (Figure 3b). Fortunately, in the MS-MRS sensor, the magnetic signal (T_2 value) is related only to the amount of target in the samples, and the stability of MB_{30} in the MS-MRS sensor is better than that of the MB_{30}-target-MB_{30} conjugate. The interassay relative standard deviation (RSD) and the intra-assay RSD were less than 8.8% and 6.5% in the MS-MRS sensor. At the same time, the interassay RSD and the intra-assay RSD were less than 14.5% and 10.8% in the conventional MRS sensor (Table S1). Therefore, the repeatability and operability of the MS-MRS sensor are superior to that of a conventional MRS sensor.

Detection of *S. enterica* in Milk. After demonstrating that the MS-MRS sensor has a better performance than ELISA and the conventional MRS assay, we applied it to the detection of *S. enterica* in real samples. Milk is essential in daily life, and it is often contaminated by *S. enterica*. We detect the *S. enterica* in milk to demonstrate the real-world application of this sensor. For comparison, we simultaneously employed the MS-MRS sensor and conventional MRS sensor for the detection (Figure 5). We set three blank samples that were determined to be free of *S. enterica* by standard culture methods (samples 1 to 3) as the negative samples. We used two approaches to detect *S. enterica* in spiked milk samples (samples 4 to 10). The MS-MRS sensor can detect 100 cfu/mL *S. enterica* in spiked samples (sample 4), while the conventional MRS sensor can detect only spiked samples with at least 10^4 cfu/mL *S. enterica*. The results from the same spiked samples indicate that MS-MRS has a better sensitivity than the conventional MRS. Finally, we detected 20 real samples (samples 11 to 30) that were identified as positive samples by real-time PCR (RT-PCR). Twelve samples are identified to be positive using our approach, while only two samples (samples 11 and 16) are identified to be positive by the conventional MRS sensor. RT-PCR is the gold standard for pathogen detection by virtue of its ultrahigh sensitivity; its sensitivity can reach 1 cfu/mL for detection of a pathogen, so that the total positive ratio is higher than that of the MS-MRS sensor. The disadvantages of PCR, however, include the long detection time (2−3 h) and high cost, which prevent it from being widely applied. The MS-MRS sensor assay can be completed in a short time (0.5 h) with convenient operation and high sensitivity, which provides an attractive platform for the detection of pathogens. Table 1 summarizes the advantages and disadvantage of ELISA, a conventional MRS sensor, and the MS-MRS sensor.

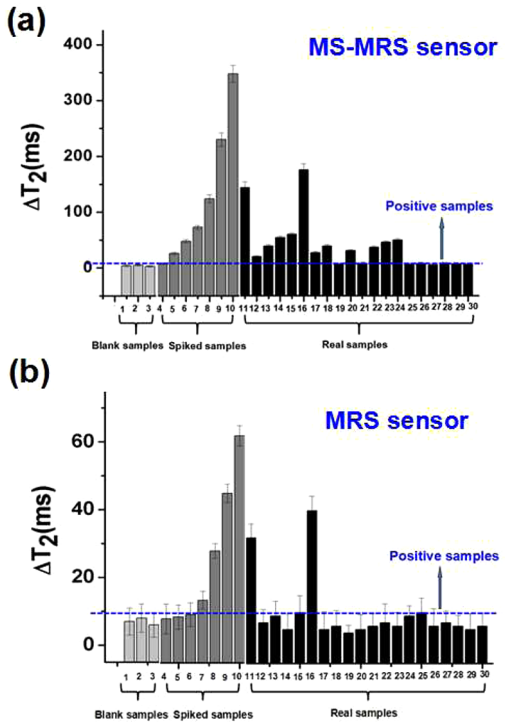

Figure 5. Results of MS-MRS for detection of blank samples, spiked samples, and real samples. (a) Results of the MS-MRS sensor for detection of *S. enterica*. (b) Results of the MRS sensor for detection of *S. enterica*. Samples 1 to 3 present normal milk from different local supermarkets; samples 4 to 10 present different concentrations of *S. enterica*-spiked samples; the final concentrations of *S. enterica* are 10, 10^2, 10^3, 10^4, 10^5, 10^6, and 10^7 cfu/mL. Samples 11 to 30 present milk from different local supermarkets proved to be positive samples by RT-PCR.

TABLE 1. Comparison between ELISA, MRS Sensor, and MS-MRS Sensor for Detection of *S. enterica*

approach	sensitivity	linear range	operation
ELISA	10^3 cfu/mL	10^4−10^6 cfu/mL	laborious
MRS sensor	10^4 cfu/mL	10^5−10^7 cfu/mL	moderate
MS-MRS sensor	10^2 cfu/mL	10^4−10^8 cfu/mL	convenient

Detection of Virus. To demonstrate the generality of MS-MRS, we chose the Newcastle disease virus (NDV) as a model for virus detection. Rapid and sensitive detection of NDV is important because NDV is highly contagious among almost all birds and mainly causes respiratory and neuronal symptoms, resulting in death.

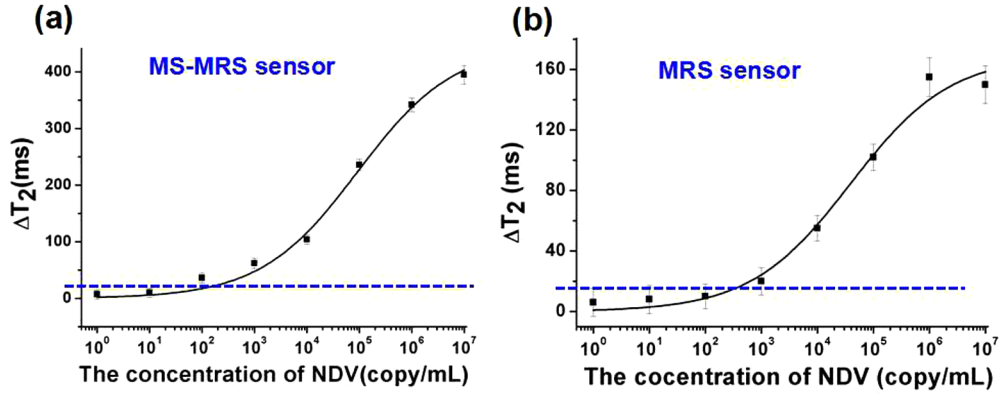

Figure 6. Result of the MRS sensor and the MS-MRS sensor for the detection of NDV. The concentration of NDV is 1, 10, 10^2, 10^3, 10^4, 10^5, 10^6, and 10^7 copy/mL. The dashed lines in (a) and (b) show the cutoff values of the MS-MRS sensor and the MRS sensor.

The results show that the LOD of a conventional MRS sensor is 10^3 copy/mL, while the LOD of the MS-MRS sensor for NDV detection is 10^2 copy/mL (Figure 6). This indicates a better sensitivity of the MS-MRS sensor for the detection of virus. A noteworthy point is that the reproducibility of our approach is better than that of a conventional MRS sensor. Researchers have studied that in conventional MRS sensing the type of targets can affect the state of MB in solution and the ΔT_2 value due to the different epitopes of the targets.[27] In our study, the ΔT_2 value relates only to the concentration of target in samples, resulting in a better performance than the conventional MRS sensor. We note that the detection range for NDV is from 10^2 to 10^7 copy/mL by MS-MRS, while the detection range for *S. enterica* is 10^2 to 10^8 cfu/mL by the same method. This difference may be due to the difference in affinity of the antibody–antigen interaction for different targets.

CONCLUSIONS

In conclusion, we develop an MRS sensing based on magnetic separation (MS-MRS) that allows for one-step, sensitive, and reproducible detection of pathogens employing the different separation speeds of MB_{30} and MB_{250} in a small magnetic field (0.01 T), and we use T_2 of the water molecules around the unreacted MB_{30} as the readout of the immunoassay. This method enables the detection of *S. enterica* in milk as well as viruses. Compared with a conventional MRS sensor, our approach shows convenient operation, enhanced sensitivity, and better reproducibility. Combined with the advantages of MRS (*i.e.*, negligible interference from biological background, simple pretreatment, and fast assay kinetics), the MS-MRS sensor can become a powerful analytic tool for molecular detection in fields such as clinical diagnosis, food safety, environmental monitoring, and so forth.

METHODS

Fabrication of MB_{250}-Ab_1 Conjugate. First, 2 mg of magnetic beads (250 nm) was suspended in 2 mL of activated buffer (80 nM MES, pH = 5.2). Then, 80 μL of EDC (10 mg mL^{-1}) and 40 μL of NHS (10 mg mL^{-1}) were added to the MB_{250} solution. After activation for about 30 min, the excess EDC, NHS, and byproducts were removed *via* magnetic separation using a magnetic scaffold; then 2 mL of PBS buffer (pH = 7.4, 0.01M) was added to resuspend the activated MB_{250}. Subsequently, 0.1 mg of capture antibody (Ab_1) was added to the activated MB_{250} solution. The mixture was gently stirred to react for 2 h at room temperature and then blocked with 1% (m/v) BSA for 0.5 h. The MB_{250}-Ab_1 conjugate was separated from the free Ab_1, resuspended in 1000 μL of PBS, and stored at 4 °C for further use.

Preparation of MB_{30}-Ab_2 Conjugate. First, 1 mg of magnetic beads MB_{30} (30 nm in diameter) was suspended in 100 μL of activated buffer (80 nM MES, pH = 6.0). Then, 10 μL of EDC (10 mg mL^{-1}) and 10 μL of NHS (10 mg mL^{-1}) were added to the MB_{30} solution. After activation for about 30 min, 1000 μL of coupling buffer PBS (pH = 7.4, 0.01 M) was added into activated MB_{30} buffer, and then 0.1 mg of detection antibody (Ab_2) was added to resuspend the activated MB_{30}. The mixture was gently stirred to react for 2 h at room temperature and then blocked with 1% (m/v) BSA for 0.5 h. The MB_{30} was separated from the free Ab_2 by SuperMag separator at 4 °C for 4 h and resuspended in 1000 μL of PBST, and then the MB_{30}-Ab_2 conjugate was separated again. Finally, it was resuspended in PBS solution (pH = 7.4, 0.01 M, 0.01% BSA) and stored at 4 °C for further use.

Process of the MS-MRS Sensor. First, 100 μL of MB_{250}-Ab_1 solution, 100 μL of MB_{30}-Ab_2 solution, and 800 μL of different concentrations of *S. enterica* (10^7, 10^6, 10^5, 10^4, 10^3, 10^2, 50, 20, 10, and 0 cfu/mL) were transferred to their individual 1.5 mL centrifuge tubes. Each mixture was gently shaken for 30 min. All the tubes were then put on a magnetic separation rack for 1 min, and 200 μL of supernatant of every tube was transferred into a 7.5 mm nuclear magnetic resonance (NMR) tube. Contents were analyzed *via* NMR for 1 min to measure T_2, and each point was assayed three times (n = 3). T_2 was acquired at a temperature of 20–35 °C using the 1.5 T NMR analysis working with ^{1}H at the 59.095 MHz magnetic field and the following parameters: Carr–Purcell–Meiboom–Gill pulse sequence, 2000 echoes, echo time of 2 ms, and repetition time of 4 s. The statistical analysis was performed using Origin 8.0 software. The limit of detection is defined as follows: the positive magnetic signal (ΔT_2) is greater than twice the background.

Process of the MRS Sensor. First, 100 μL of MB_{30}-Ab_2 solution and 900 μL of different concentrations of *S. enterica* (10^7, 10^6, 10^5, 10^4, 10^3, 10^2, 50, 20, 10, and 0 cfu/mL) were transferred to their respective 1.5 mL centrifuge tubes. Each mixture solution was gently shaken for 30 min. Then, 200 μL of mixture solution

was transferred into a 7.5 mm NMR tube for measurement of T_2 value *via* NMR analysis, and each point was assayed three times (n = 3). T_2 was acquired at a temperature of 20−35 °C using the 1.5 T NMR analysis working with ^{1}H at the 59.095 MHz magnetic field and the following parameters: Carr−Purcell−Meiboom−Gill pulse sequence, 2000 echoes, echo time of 2 ms, and repetition time of 4 s. The statistical analysis used Origin 8.0 software.

Conflict of Interest: The authors declare no competing financial interest.

Supporting Information Available: This material is available free of charge *via* the Internet at http://pubs.acs.org.

Acknowledgment. We thank the Ministry of Science and Technology of China (2011CB933201 and 2013YQ190467), the National Science Foundation of China (21025520, 21105018, 21222502, 91213305, and 21475028), Chinese Academy of Sciences (XDA09030305), and the Capital Health Research and Development of Special (No. 2011-1003-02) for financial support. We also thank the Shanghai Shinning Globe Science and Education Equipment Co., Ltd (Shanghai, China), for providing a 1.5 T NMR analysis for measurement of T_2.

REFERENCES AND NOTES

1. Chen, W. W.; Li, Q. Z.; Zheng, W. S.; Hu, F.; Zhang, G. X.; Wang, Z.; Zhang, D. Q.; Jiang, X. Y. Identification of Bacteria in Water by a Fluorescent Array. *Angew. Chem., Int. Ed.* **2014**, *53*, 13734–13739.
2. Zhang, Y.; Zhang, L.; Sun, J. S.; Liu, Y. L.; Ma, X. J.; Cui, S. J.; Ma, L. Y.; Xi, J. J.; Jiang, X. Y. Point-of-Care Multiplexed Assays of Nucleic Acids Using Microcapillary-Based Loop-Mediated Isothermal Amplification. *Anal. Chem.* **2014**, *86*, 7057–7062.
3. Xianyu, Y. L.; Wang, Z.; Jiang, X. Y. A Plasmonic Nanosensor for Immunoassay *via* Enzyme-Triggered Click Chemistry. *ACS Nano* **2014**, *8*, 12741–12747.
4. Irwansyah, I.; Li, Y. Q.; Shi, W. X.; Qi, D. P.; Leow, W. R.; Tang, M. B. Y.; Li, S. Z.; Chen, X. D. Gram-Positive Antimicrobial Activity of Amino Acid-Based Hydrogels. *Adv. Mater.* **2015**, *27*, 648–654.
5. Du, J. J.; Zhu, B. W.; Peng, X. J.; Chen, X. D. Optical Reading of Contaminants in Aqueous Media Based on Gold Nanoparticles. *Small* **2014**, *10*, 3461–3479.
6. Li, Y. Q.; Zhu, B. W.; Li, Y. G.; Leow, W. R.; Goh, R.; Ma, B.; Fong, E.; Tang, M.; Chen, X. D. A Synergistic Capture Strategy for Enhanced Detection and Elimination of Bacteria. *Angew. Chem., Int. Ed.* **2014**, *53*, 5837–5841.
7. Tao, Y.; Ran, X.; Ren, J. S.; Qu, X. G. Array-Based Sensing of Proteins and Bacteria by Using Multiple Luminescent Nanodots as Fluorescent Probes. *Small* **2014**, *10*, 3667–3671.
8. Terao, Y.; Yonekita, T.; Morishita, N.; Fujimura, T.; Matsumoto, T.; Morimatsu, F. Potential Rapid and Simple Lateral Flow Assay for Escherichia coli O111. *J. Food Prot.* **2013**, *76*, 755–761.
9. Kim, T. H.; Park, J.; Kim, C. J.; Cho, Y. K. Fully Integrated Lab-on-a-Disc for Nucleic Acid Analysis of Food-Borne Pathogens. *Anal. Chem.* **2014**, *86*, 3841–3848.
10. Crannell, Z. A.; Castellanos-Gonzalez, A.; Irani, A.; Rohrman, B.; White, A. C.; Richards-Kortum, R. Nucleic Acid Test to Diagnose Cryptosporidiosis: Lab Assessment in Animal and Patient Specimens. *Anal. Chem.* **2014**, *86*, 2565–2571.
11. Perez, J. M.; Simeone, F. J.; Saeki, Y.; Josephson, L.; Weissleder, R. Viral-Induced Self-Assembly of Magnetic Nanoparticles Allows the Detection of Viral Particles in Biological Media. *J. Am. Chem. Soc.* **2003**, *125*, 10192–10193.
12. Yang, K. S.; Budin, G.; Reiner, T.; Vinegoni, C.; Weissleder, R. Bioorthogonal Imaging of Aurora Kinase A in Live Cells. *Angew. Chem., Int. Ed.* **2012**, *51*, 6598–6603.
13. Chung, H. J.; Castro, C. M.; Im, H.; Lee, H.; Weissleder, R. A Magneto-DNA Nanoparticle System for Rapid Detection and Phenotyping of Bacteria. *Nat. Nanotechnol.* **2013**, *8*, 369–375.
14. Ling, Y.; Pong, T.; Vassiliou, C. C.; Huang, P. L.; Cima, M. J. Implantable Magnetic Relaxation Sensors Measure Cumulative Exposure to Cardiac Biomarkers. *Nat. Biotechnol.* **2011**, *29*, 273–277.
15. Liu, D. S.; Tangpeerachaikul, A.; Selvaraj, R.; Taylor, M. T.; Fox, J. M.; Ting, A. Y. Diels-Alder Cycloaddition for Fluorophore Targeting to Specific Proteins inside Living Cells. *J. Am. Chem. Soc.* **2012**, *134*, 792–795.
16. Tsourkas, A.; Hofstetter, O.; Hofstetter, H.; Weissleder, R.; Josephson, L. Magnetic Relaxation Switch Immunosensors Detect Enantiomeric Impurities. *Angew. Chem., Int. Ed.* **2004**, *43*, 2395–2399.
17. Koh, I.; Hong, R.; Weissleder, R.; Josephson, L. Nanoparticle-Target Interactions Parallel Antibody-Protein Interactions. *Anal. Chem.* **2009**, *81*, 3618–3622.
18. Perez, J. M.; Josephson, L.; O'Loughlin, T.; Hogemann, D.; Weissleder, R. Magnetic Relaxation Switches Capable of Sensing Molecular Interactions. *Nat. Biotechnol.* **2002**, *20*, 816–820.
19. Peterson, V. M.; Castro, C. M.; Lee, H.; Weissleder, R. Orthogonal Amplification of Nanoparticles for Improved Diagnostic Sensing. *ACS Nano* **2012**, *6*, 3506–3513.
20. Tassa, C.; Shaw, S. Y.; Weissleder, R. Dextran-Coated Iron Oxide Nanoparticles: A Versatile Platform for Targeted Molecular Imaging, Molecular Diagnostics, and Therapy. *Acc. Chem. Res.* **2011**, *44*, 842–852.
21. Min, C.; Shao, H.; Liong, M.; Yoon, T.-J.; Weissleder, R.; Lee, H. Mechanism of Magnetic Relaxation Switching Sensing. *ACS Nano* **2012**, *6*, 6821–6828.
22. Lee, H.; Sun, E.; Ham, D.; Weissleder, R. Chip-NMR Biosensor for Detection and Molecular Analysis of Cells. *Nat. Med.* **2008**, *14*, 869–874.
23. Issadore, D.; Min, C.; Liong, M.; Chung, J.; Weissleder, R.; Lee, H. Miniature Magnetic Resonance System for Point-of-Care Diagnostics. *Lab Chip* **2011**, *11*, 2282–2287.
24. Haun, J. B.; Devaraj, N. K.; Hilderbrand, S. A.; Lee, H.; Weissleder, R. Bioorthogonal Chemistry Amplifies Nanoparticle Binding and Enhances the Sensitivity of Cell Detection. *Nat. Nanotechol.* **2010**, *5*, 660–665.
25. Liong, M.; Fernandez-Suarez, M.; Issadore, D.; Min, C.; Tassa, C.; Reiner, T.; Fortune, S. M.; Toner, M.; Lee, H.; Weissleder, R. Specific Pathogen Detection Using Bioorthogonal Chemistry and Diagnostic Magnetic Resonance. *Bioconjugate Chem.* **2011**, *22*, 2390–2394.
26. Colombo, M.; Sommaruga, S.; Mazzucchelli, S.; Polito, L.; Verderio, P.; Galeffi, P.; Corsi, F.; Tortora, P.; Prosperi, D. Site-Specific Conjugation of ScFvs Antibodies to Nanoparticles by Bioorthogonal Strain-Promoted Alkyne-Nitrone Cycloaddition. *Angew. Chem., Int. Ed.* **2012**, *51*, 496–499.
27. Kaittanis, C.; Santra, S.; Santiesteban, O. J.; Henderson, T. J.; Perez, J. M. The Assembly State between Magnetic Nanosensors and Their Targets Orchestrates Their Magnetic Relaxation Response. *J. Am. Chem. Soc.* **2011**, *133*, 3668–3676.
28. Kaittanis, C.; Santra, S.; Perez, J. M. Role of Nanoparticle Valency in the Nondestructive Magnetic-Relaxation-Mediated Detection and Magnetic Isolation of Cells in Complex Media. *J. Am. Chem. Soc.* **2009**, *131*, 12780–12791.
29. Junillon, T.; Mosticon, D.; Mallen, B.; Baril, F.; Morand, L.; Michel, D.; Flandrois, J. P. Optimization of the Reactional Medium and a Food Impact Study for a Colorimetric *in Situ* Salmonella spp. Detection Method. *Int. J. Food Microbiol.* **2014**, *181*, 48–52.
30. Laube, T.; Cortes, P.; Llagostera, M.; Alegret, S.; Pividori, M. I. Phagomagnetic Immunoassay for the Rapid Detection of Salmonella. *Appl. Microbiol. Biotechnol.* **2014**, *98*, 1795–1805.